

# Computational screening of doping schemes for $\text{LiTi}_2(\text{PO}_4)_3$ as cathode coating materials\*

Yu-Qi Wang(王宇琦)<sup>1,2</sup>, Xiao-Rui Sun(孙晓瑞)<sup>1,2</sup>, Rui-Juan Xiao(肖睿娟)<sup>1,2,†</sup>, and Li-Quan Chen(陈立泉)<sup>1,2</sup>

<sup>1</sup>Beijing Advanced Innovation Center for Materials Genome Engineering, Institute of Physics, Chinese Academy of Sciences, Beijing 100190, China

<sup>2</sup>University of Chinese Academy of Sciences, Beijing 100190, China

(Received 29 November 2019; revised manuscript received 15 January 2020; accepted manuscript online 30 January 2020)

In all-solid-state lithium batteries, the impedance at the cathode/electrolyte interface shows close relationship with the cycle performance. Cathode coatings are helpful to reduce the impedance and increase the stability at the interface effectively.  $\text{LiTi}_2(\text{PO}_4)_3$  (LTP), a fast ion conductor with high ionic conductivity approaching  $10^{-3} \text{ S}\cdot\text{cm}^{-1}$ , is adopted as the coating materials in this study. The crystal and electronic structures, as well as the  $\text{Li}^+$  ion migration properties are evaluated for LTP and its doped derivatives based on density functional theory (DFT) and bond valence (BV) method. Substituting part of Ti sites with element Mn, Fe, or Mg in LTP can improve the electronic conductivity of LTP while does not decrease its high ionic conductivity. In this way, the coating materials with both high ionic conductivities and electronic conductivities can be prepared for all-solid-state lithium batteries to improve the ion and electron transport properties at the interface.

**Keywords:** lithium battery materials, high-throughput calculations, density functional theory, virtual screening

**PACS:** 82.47.Aa, 31.15.es

**DOI:** [10.1088/1674-1056/ab7186](https://doi.org/10.1088/1674-1056/ab7186)

## 1. Introduction

With the development of industry and technology, there is an increasing requirement on the performance of energy and power devices in the world.<sup>[1]</sup> Meanwhile, the burning of fossil fuel and biomass energy releases greenhouse gases such as carbon dioxide, methane, and so on, which raises the problem of global warming.<sup>[2]</sup> As a result, lots of studies on environmentally friendly energies have been taken and made great progress, including solar energy, wind energy, geothermal energy, etc.<sup>[3]</sup> In order to store these new energies, we need to find new devices meeting the environmental constraints. The lithium rechargeable battery is a preferred option. Since John B. Goodenough firstly developed  $\text{LiCoO}_2$  as the cathode of Li ion rechargeable batteries in 1980s and it was applied by Sony in its first commercial Li ion battery, people have been trying their best to improve the properties of the Li batteries.<sup>[4,5]</sup> All-solid-state lithium battery has attracted much attention as an energy storage device because of its higher chemical stability, higher safety, and higher energy density compared with traditional lithium-ion batteries with liquid electrolyte.<sup>[6]</sup> However the impedance at the interface between the electrode and solid-state electrolyte (SSE) is usually high, which will degrade the properties of the battery.<sup>[7]</sup> Three reasons have been realized for such high impedance: (a) the diffusion and interface reac-

tion between SSE/electrolyte; (b) the chemical decomposition of the interface of SSE/electrolyte during cycling; (c) the bad invasion and volume changing during cycling induce the poor contact between SSE/electrolyte.<sup>[8]</sup> Coating has been proved as an effective way to increase the interfacial stability and decrease the impedance.<sup>[9]</sup> In this work, the doping scheme for the fast ion conductor  $\text{LiTi}_2(\text{PO}_3)_4$  (LTP) is investigated theoretically, aiming to discover new coating materials with both good ionic and electronic transport properties.

NASICON-typed  $\text{LiTi}_2(\text{PO}_3)_4$  belongs to the rhombohedral crystal system.<sup>[10]</sup> In its lattice, the octahedron  $\text{TiO}_6$  shares all the corners with the tetrahedron  $\text{PO}_4$ , and the alkali metal ions  $\text{Li}^+$  are located between them. The conductive channels are formed in the space connected by the lattice sites of the alkali metal ions and the interstitial sites, and the alkali metal ions are easily transmitted along these three-dimensional channels,<sup>[11]</sup> resulting in the high ionic conductivity approaching  $10^{-3} \text{ S}\cdot\text{cm}^{-1}$ .<sup>[12]</sup> However, LTP is electrically insulating, which blocks the electronic transportation among the cathode particles. Doping is regarded as an effective way to adjust the electronic structure,<sup>[13]</sup> thus it is adopted to create LTP-derivatives with improved electronic conductivity.

High-throughput computation has been adopted to search

\*Project supported by the National Natural Science Foundation of China (Grant No. 51772321), and the National Key R&D Program of China (Grant No. 2017YFB0701602), and the Youth Innovation Promotion Association, China (Grant No. 2016005). The Shanghai Supercomputer Center provided the computing resources.

†Corresponding author. E-mail: [rjxiao@iphy.ac.cn](mailto:rjxiao@iphy.ac.cn)

for materials with the appropriate properties for cathode coatings,<sup>[7]</sup> in which  $\text{LiH}_2\text{PO}_4$ ,  $\text{LiTi}_2(\text{PO}_4)_3$ , and  $\text{LiPO}_3$  are assigned as appealing candidates from 104082 Li-containing compounds according to the phase stability, electrochemical stability, and chemical stability. In this work, we screen the doping schemes of LTP to find cathode coating materials based on density functional theory (DFT)<sup>[14]</sup> and bond valence theory (BV).<sup>[15,16]</sup> We look for the schemes that not only improve the electronic conductivity but also can not seriously reduce the ionic conductivity. First of all, we choose 13 kinds of elements to replace 25% of Ti sites in the LTP crystal cell, the crystal and electronic structures are simulated by DFT calculations and the  $\text{Li}^+$  migration pathways and activation barriers are evaluated by the BV method. Besides, elements N and S are used to replace 4.17% of the O sites in LTP respectively. The energy band gap and the migration energy barrier for each substitution scheme are obtained to evaluate the effect of doping on the electronic and ionic transport properties. Aiming at improving the electronic conductivity of LTP, we are fond of the doping systems that can introduce electron carriers or narrow the energy gap, and the devotion of doping elements to the electronic conductivity is estimated. The substitution of Mn, Fe, or Mg at part of the Ti sites is assigned as promising schemes.

## 2. Method

A rhombohedral cell is adopted to simulate the doping effects in LTP. As shown in Fig. 1, there are 4 Ti sites and 24 O sites in the cell, and the two inequivalent O sites are labeled as O1 and O2, respectively. Only one site of Ti or O is replaced by other elements. The total energies are calculated based on the first-principles DFT method using Vienna *ab initio* simulation package (VASP)<sup>[17]</sup> with the projector augmented wave (PAW) method.<sup>[18]</sup> The exchange correlation functional is chosen as the generalized gradient approximation (GGA).<sup>[19]</sup> Furthermore, when transition metal elements such as Ti, Mn, Fe, Co, Ni, and Nb are involved, we use the GGA +*U* to better describe the exchange–correlation of the transition metal

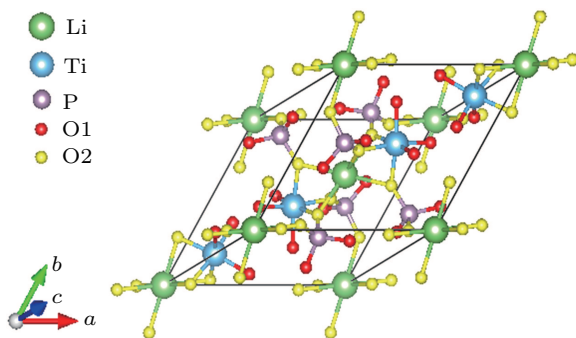


Fig. 1. Crystal cell of LTP. The green, blue, purple, red, and yellow balls represent Li, Ti, P, O1, and O2 sites, respectively.

oxides. The values of *U* we adopted are 0 eV (Ti), 3.9 eV (Mn), 5.3 eV (Fe), 3.3 eV (Co), 6.2 eV (Ni), and 0 eV (Nb). The cutoff energy is chosen as 900 eV and the *k*-point sampling mesh is  $3 \times 3 \times 3$ . Both ions and cells are relaxed in the optimization with the energy and force convergence criteria of  $10^{-5}$  eV and 0.01 eV/Å, respectively. After the relaxed crystal structures are obtained by DFT calculations, the BV simulation is carried out to extract the  $\text{Li}^+$  migration pathways and energy barriers. Only the candidates with band gap and energy barrier lower than screening criteria are left.

## 3. Results

To identify the proper candidates, we consider three factors: (a) doping should not increase the ionic activation energy seriously; (b) doping should vanish or narrow the energy gap at the Fermi energy; (c) doping should make obvious contribution to improve the electronic conduction.

### 3.1. Activation energy

The BV theory can estimate the ionic conduction property according to the crystal structure and represent it by pathways and energy barriers. In this method, the total potential energy *E* for each virtual Li site is defined as<sup>[14]</sup>

$$E = D_0 \left\{ (\exp[\alpha(R_{\min} - R)])^2 - 1 \right\} + \frac{q_{\text{Li}}q_A}{R_{\text{Li}-A}} \operatorname{erfc}\left(\frac{R_{\text{Li}-A}}{\rho_{\text{Li}-A}}\right). \quad (1)$$

Here, *E* consists of two parts. The first part originates from the attraction between  $\text{Li}^+$  and its bonding anions. Thereinto,  $\alpha$ ,  $R_{\min}$ ,  $D_0$  are experience parameters describing the bonding interactions and *R* is the real bond length in the structure.  $R_{\min}$  is determined by

$$R_{\min} = R_0 \times [0.9185 + 0.2285|\sigma_A - \sigma_X|] - b \ln\left(\frac{V_{\text{id}}}{N_c}\right), \quad (2)$$

where  $N_c$  is the coordination number of the central atom,  $V_{\text{id}}$  is the oxidation value of the central atom, and the part in bracket involves the polarization ( $\sigma_A$  and  $\sigma_X$  are the complete softness of cation and anion) and the influence of other coordination shells.  $D_0$  is determined by

$$D_0 = \frac{kb^2}{2} = c \times \left(14.4 \frac{\text{eV}}{\text{\AA}}\right) \frac{[V_{\text{id}}(A)V_{\text{id}}(X)]^{1/c} b^2}{R_{\min} \sqrt{n_A n_X}}. \quad (3)$$

If the restrictive factor of cation comes from s or p shells,  $c = 1$ ; if the restrictive factor comes from d or f shells,  $c = 2$ .  $n_A$  and  $n_X$  are the intrinsic quantum numbers of cation A and anion X, respectively.  $V_{\text{id}}(A)$  and  $V_{\text{id}}(X)$  are the absolute values of nominal charge. The second part originates from the exclusion between  $\text{Li}^+$  and other unmoved cations.  $\rho_{\text{Li}-A} = (r_{A1} + r_{A2})f \approx 2 \text{\AA}$ .  $r_{A1}$  and  $r_{A2}$  are the covalent radii. Factor *f* depends on the average absolute cation electronegativity and the average cation charge in the compound and *f*

ranges in  $0.74 \pm 0.04$ .<sup>[15]</sup> Assuming that there is one  $\text{Li}^+$  ion situated at each site of a dense mesh in the crystal cell, the energy landscape of  $\text{Li}^+$  in the cell can be calculated. The smallest critical energy at which an isosurface with connective channels forms in the whole structure is taken as the activation energy barrier for  $\text{Li}^+$  migration. According to the shapes of the channels, we can classify the transportation characteristics into 1-, 2-, or 3-dimension (1D, 2D, or 3D).

The BV-method-calculated  $\text{Li}^+$  activation energy of LTP is 0.87 eV. The corresponding ionic migration channels are 3D and shown in Fig. 2. The  $\text{Li}^+$  migration energy barriers for various doping schemes are illustrated in Fig. 3. Doping with the elements Ni, Zr, Bi, Nb decreases the activation energy to 0.72 eV, 0.79 eV, 0.83 eV, 0.86 eV, respectively, declaring that the introducing of these elements improves the  $\text{Li}^+$  migration. The ionic activation energies of the rest schemes are all increased and the activation energies with different doping elements are sorted as  $\text{Ga} > \text{Fe} > \text{Co} = \text{Ge} = \text{Mg} > \text{Sn} > \text{Mn} > \text{Al} > \text{Si}$ . However, even the highest barrier, which is found in the Ga-doped case, is increased by less than 20% compared with the barrier in LTP. Therefore, the doping at the Ti site seems not to influence the ionic transport properties seriously.

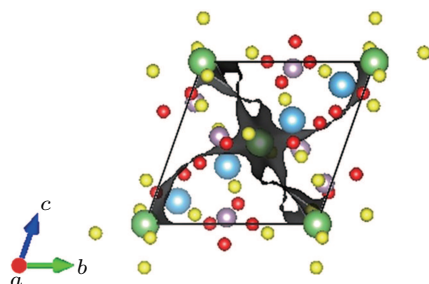


**Fig. 2.** The ionic migration channels of LTP. The black isosurface with the isovalue of 0.87 eV indicates the  $\text{Li}^+$  migration pathways, which show 3D characteristics.

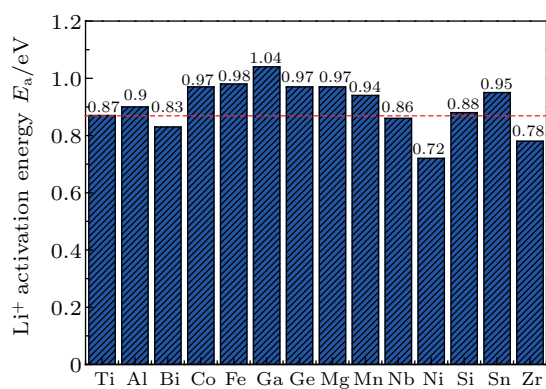


**Fig. 3.**  $\text{Li}^+$  migration activation energies for various Ti-site doping schemes in LTP. The horizontal axis represents the doped elements and the energy barrier of LTP is shown for comparison.

The  $\text{Li}^+$  activation energies for the doping at O sites are also simulated. According to the total energies calculated by

DFT method, the structures doped at O2 site are more stable than those doped at O1 site, then the stable crystal structures are transferred to BV calculations. The results indicate that substituting one oxygen atom at O2 site with N and S will increase the  $\text{Li}^+$  migration energy barrier to 1.57 eV and 1.06 eV, respectively. The introduction of N into O site seems to obstacle the  $\text{Li}^+$  migration greatly, while replacing one oxygen atom by sulfur will not deteriorate the ionic transportation much.

### 3.2. Electronic band structures

According to the DFT calculations, LTP is a semiconductor with an energy gap of 2.27 eV. The electronic structures of the doped systems are also evaluated by DFT method. The effects of doping on the electronic structures are illustrated in Fig. 4. The effects of Ti-site doping on the band structures can be classified into 4 typical types. In Fig. 4(a), the Fermi level shifts to the lower energy side, and some hole carriers are created. The substitution of Ti by Al, Bi, Co, Fe, Ga, Mg, and Mn causes similar effect on the electronic structure as shown in Fig. 4(a). In this case, the band gap is vanished and the electronic conductivity is improved. The second case is shown in Fig. 4(b), the Fermi level shifts to the higher energy side and electron carriers are formed. Only the substitution of Nb for one Ti-site belongs to this case, and the electronic conductivity is expected to increase because of the vanishing of band gap and forming of carriers. The third case is shown in Fig. 4(c), the impurity energy levels are formed and the energy gap is narrowed, which is also helpful to improve the electronic conductivity. The substitution of Ni for Ti-site belongs to the third case, and the energy gap decreases to 0.44 eV. The last case is shown in Fig. 4(d), in which the energy gap is broadened and the electronic conductivity is expected to decrease. Replacing one Ti-site with Ge, Si, Sn, Zr will cause such kind of effect on the electronic structures, and these doping schemes have no positive influence on the electronic conductivity, thus they will not be considered later.

We also calculate the electronic band structures for N- and S-doped O site in LTP, and the results are shown in Fig. 5. When replacing one of the O2 sites by N, the Fermi level moves towards the low energy side and hole carriers are created, which is expected to improve the electronic conductivity. However, if one of the O2 sites is replaced by S, it only narrows the energy gap to 1.37 eV. Although doping one of the O2 sites with N is hopeful to improve the electronic conductivity, the  $\text{Li}^+$  ion migration pathways are blocked by the doped ion, which prevents the application of the N-doping scheme.

Based on the above analysis, 9 elements, Al, Bi, Co, Fe, Ga, Mg, Mn, Nb, and Ni, are chosen to replace part of Ti sites in LTP, which are promising strategies to improve the electronic conductivity without obvious deterioration of the ionic conductivity.

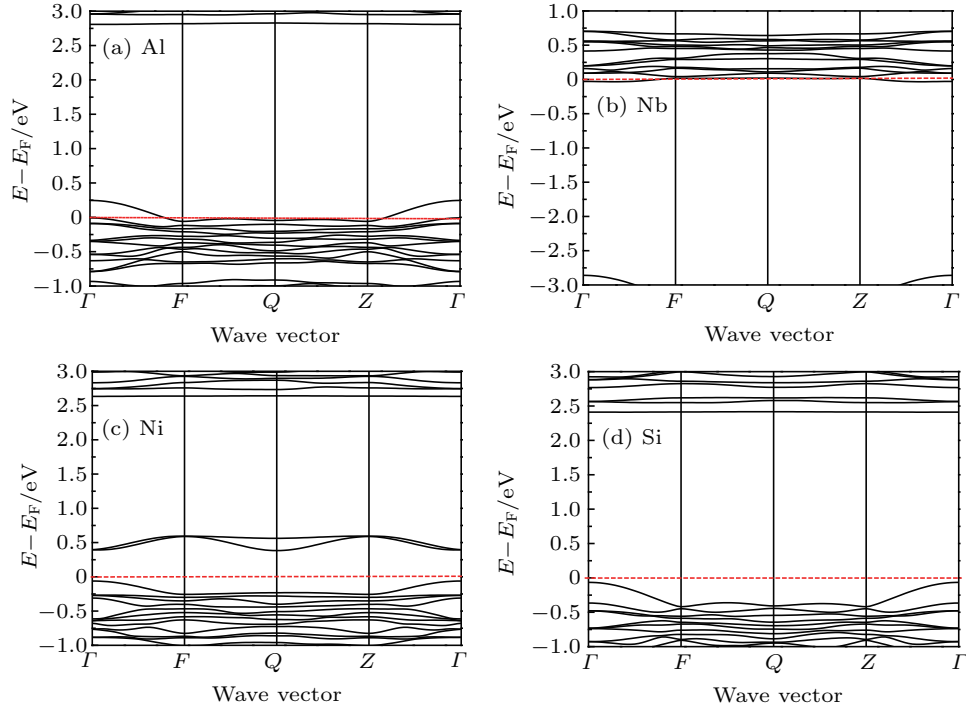


**Fig. 4.** Electronic band structures for typical doping schemes in which one Ti site is replaced by (a) Al, (b) Nb, (c) Ni, and (d) Si. The dotted line presents the Fermi level.

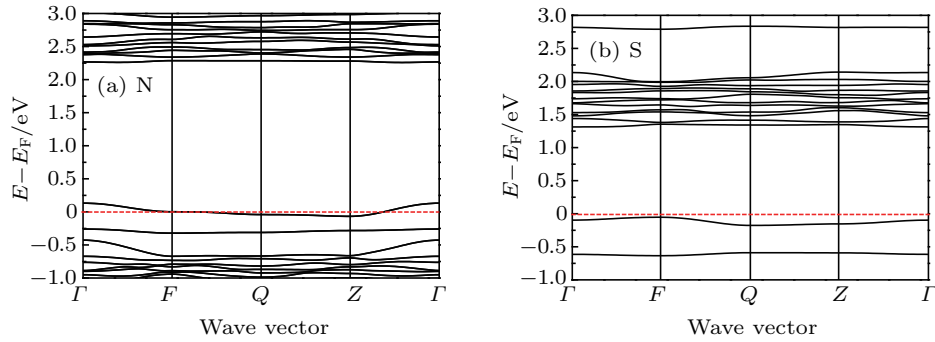


**Fig. 5.** Electronic band structures of doping schemes in which one O site is replaced by (a) N and (b) S. The dotted line presents the Fermi level.

### 3.3. Density of states

According to the above screening process, we have chosen 9 doping schemes which may contribute to improve the electronic conductivity. We attempt to quantify the doping effect by estimate the electronic conductivity in each case according to the density of states (DOS). The DOS near the Fermi level of these 9 doping schemes is shown in Fig. 6. It is known that the electronic conductivity is related with the carrier concentration and the electronic effective mass as

$$\sigma_e = \frac{ne^2\tau}{m^*}, \quad (4)$$

where  $n$  is the density of carriers,  $e$  is the elementary charge,  $\tau$  is the relaxation time, and  $m^*$  is the electronic effective mass.  $\tau$  is related to many factors including temperature and it ranges from  $10^{-13}$  s to  $10^{-14}$  s at room temperature. The accurate calculation of  $\tau$  needs building a proper model and here we take

$\tau$  as an invariable parameter here. In solid state physics, the electronic effective mass is obtained as

$$m^* = \left( \frac{1}{\hbar^2} \frac{\partial^2 E}{\partial^2 k} \right)^{-1}, \quad (5)$$

where  $E$  is the energy and  $k$  is the wave vector.  $m^*$  varies in a small range, so the density of carriers plays a primary role on the electronic conductivity in LTP-doped systems. The concentration of hole or electron carriers can be estimated by integrating the DOS near the Fermi level,

$$n = \frac{1}{V} \int g(E) dE. \quad (6)$$

According to Fig. 6, we can see that doping with element Mn, Fe, or Mg will introduce more carriers than the other cases. Doping with element Al or Ga contributes less to the introduction of carriers. While doping with element Bi, Co, Nb, or Ni makes negligible contribution to the carrier formation.

For clarity, the partial density of states for Mn, Fe, Mg, and Bi doped systems is shown in Fig. 7 to provide more details. The doped atoms bonded with O atoms around them and bring an extra peak at the Fermi level when the doped element is Mn, Fe, or Mg. The effects of other schemes are similar to that of Bi, in which the amount of carriers increases slightly. As a result, 3 doping schemes, which are doping one of the Ti sites with Mn, Fe, or Mg, are further screened out from the 9 candidate strategies because they will improve the electronic conductivity more effectively.

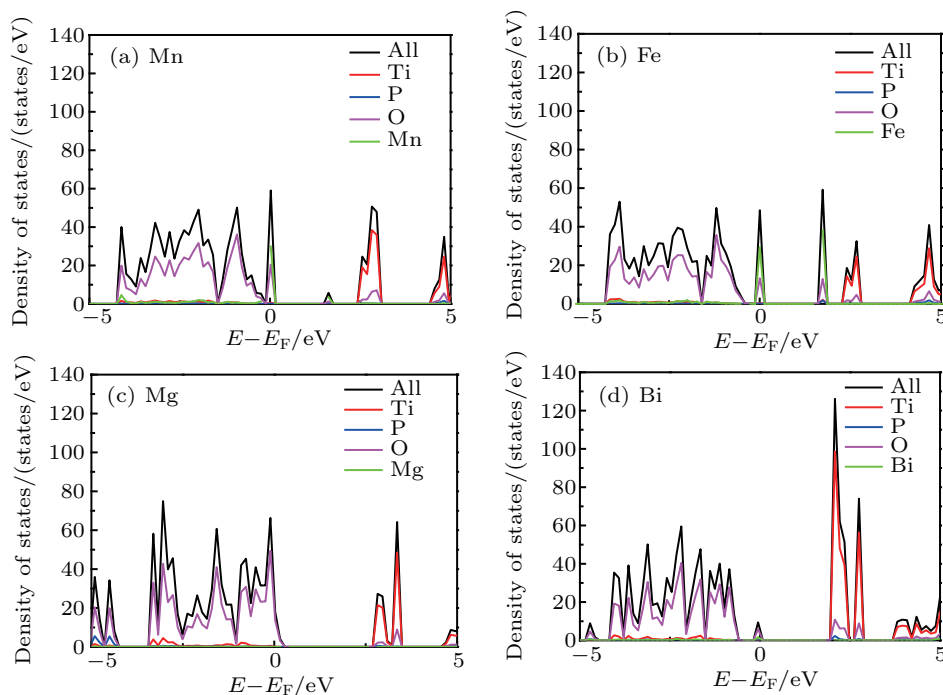


Fig. 7. Partial density of states for (a) Mn-, (b) Fe-, (c) Mg-, or (d) Bi-doping at one of the Ti sites.

#### 4. Discussion

To further understand the effects related with the doping schemes, the local structures of the doped systems are analyzed. Replacing one of the Ti sites in LTP does not influence its structural parameters seriously. Doping changes the lattice size and bond lengths in LTP. Figure 8 shows the relationship between the radius of the doped ions and the lattice parameter  $a$  of the doped structures. A linear correlation between the above two variables can be found. We also notice that replacing O sites in LTP brings more obvious impact on both structures and migration properties, because it will change the chemical environments around the migration ions directly. As to the ionic conductivity, replacing one of the Ti sites in LTP does not change the  $\text{Li}^+$  migration activation energy obviously. It is because Ti is located in the center of octahedron and replacing the center atom makes indirect impact

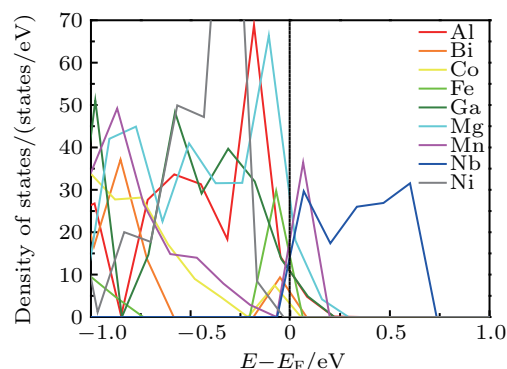
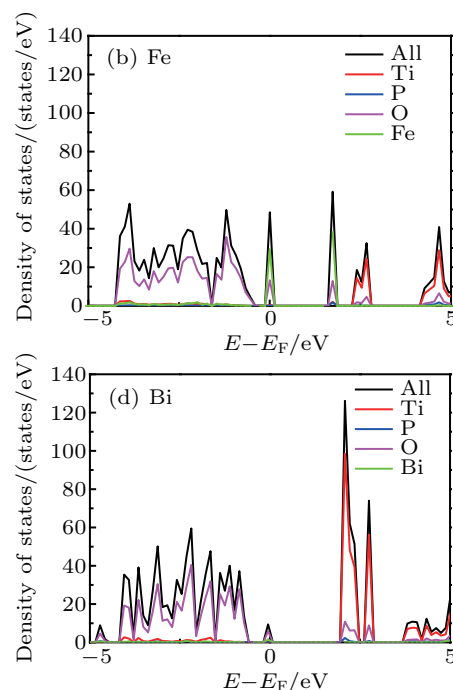


Fig. 6. Density of states near the Fermi level for 9 doping schemes at one of the Ti sites.



on the structures outside the polyhedron. Thus the  $\text{Li}^+$  ion migration channels are not destroyed. However, replacing one of the O sites in LTP will distort the initial octahedron badly and introduce direct influence on the  $\text{Li}^+$  migration pathways near to the doped atom, which decreases the  $\text{Li}^+$  ionic conductivity.

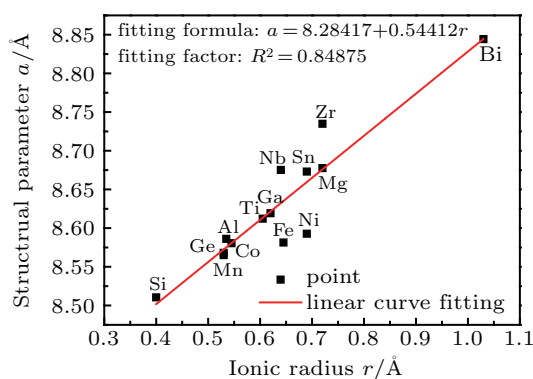


Fig. 8. Relationship between the radius of the doped ions and the size of their doped structures.

## 5. Summary

We have calculated the structures and properties of LTP and its doped derivatives based on DFT and BV theory. LTP has high ionic conductivity but is electrically insulating. Replacing 25% of Ti sites in LTP with elements Mn, Fe, or Mg can improve the electronic conductivity of LTP while maintain its high ionic conductivity. And then the doped LTP is hopefully used as a cathode coating material to provide both high ionic conductivity and good electronic conductivity. To realize the application of these candidates, further investigations on the electrochemical stability of the doped-LTP materials and the chemical stability between cathodes and coatings should be considered in the future.

## References

- [1] Etacheri V, Marom R, Elazari R, Salitra G and Aurbach D 2011 *Energy & Environ. Sci.* **4** 3243
- [2] Poizot P and Dolhem F 2011 *Energy & Environ. Sci.* **4** 2003
- [3] Jacobson M Z and Delucchi M A 2011 *Ene. Policy* **39** 1154
- [4] Mizushima K, Jones P C, Wiseman P J and Goodenough J B 1980 *Mater. Res. Bull.* **15** 783
- [5] Li H, Wang Z, Chen L and Huang X 2009 *Adv. Mater.* **21** 4593
- [6] Yao X Y, Liu D, Wang C S, Long P, Peng G, Hu Y S, Hu Y S, Li H, Chen L Q and Xu X X 2016 *Nano Lett.* **16** 7148
- [7] Xiao Y, Miara L J, Wang Y and Ceder G 2019 *Joule* **3** 1
- [8] Wang Q Y, Wang S, Zhang J N, Zheng J Y, Yu X Q and Li H 2017 *Energy Storage Science and Technology* **6** 1008
- [9] He Y, Yu X Q, Wang Y H, Li H and Huang X J 2011 *Adv. Mater.* **23** 4938
- [10] Aatiq A, Ménétrier M, Croguennec L, Suardec E and Delmas C 2002 *J. Mater. Chem.* **12** 2971
- [11] Lu X, Wang S H, Xiao R J, Shi S Q, Li H and Chen L Q 2017 *Nano Energy* **41** 626
- [12] Takada K, Tansho M, Yanase I, Inada T and Kajiyama A 2001 *Solid State Ionics* **139** 241
- [13] Chen Z, Qin Y, Amine K and Sun Y K 2010 *J. Mater. Chem.* **20** 7606
- [14] Hohenberg P and Kohn W 1964 *Phys. Rev. B* **136** B864
- [15] Adams S and Rao R P 2011 *Phys. Status Solidi A* **208** 1746
- [16] Xiao R J, Li H and Chen L Q 2015 *Sci. Rep.* **5** 14227
- [17] Kresse G and Furthmüller J 1996 *Comput. Mater. Sci.* **6** 15
- [18] Blochl P E 1994 *Phys. Rev. B* **50** 17953
- [19] Perdew J P, Burke K and Ernzerhof M 1996 *Phys. Rev. Lett.* **77** 3865